DTU Library

Methanol Promoted Oxidation of Nitrogen Oxide (NOx) by Encapsulated Ionic Liquids (ENILs)

Santiago, Ruben; Mossin, Susanne; Bedia, Jorge; Fehrmann, Rasmus; Palomar, José

Sustainability Engineering and Green Chemistry

Methanol Promoted Oxidation of Nitrogen Oxide (NOx) by Encapsulated Ionic Liquids (ENILs)

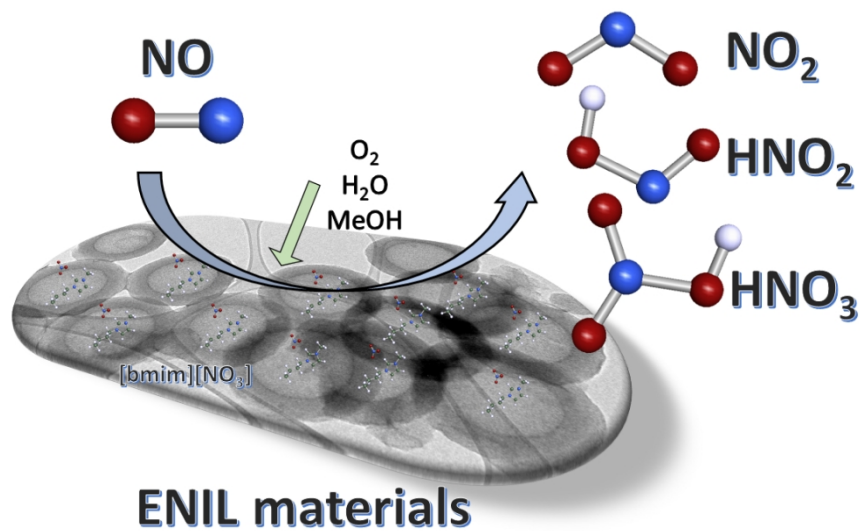Ruben Santiago, Susanne Mossin, Jorge Bedia, Rasmus Fehrmann, and José Palomar

Just Accepted

Environmental Science & Technology

Methanol promoted oxidation of NO using Encapsulated Ionic Liquids (ENILs)

338x190mm (96 x 96 DPI)

1   **Methanol Promoted Oxidation of Nitrogen Oxide (NO$_x$)**

2   **by Encapsulated Ionic Liquids (ENILs)**

3   Rubén Santiago[1*], Susanne Mossin[2], Jorge Bedia[1], Rasmus Fehrmann[2], and

4   José Palomar[1]

5   [1]*Chemical Engineering Department. Universidad Autónoma de Madrid. 28049 Madrid.*

6   *Spain*

7   [2]*Centre for Catalysis and Sustainable Chemistry, Department of Chemistry, Technical*

8   *University of Denmark, DK-2800 Kgs. Lyngby (Denmark).*

9   Corresponding author: ruben.santiago@uam.es

10   **Keywords**: NO oxidation; NO$_x$ removal; Ionic Liquids; ENIL; Flue gas

11   **Abstract**

12   The removal of nitrogen oxides (NO$_x$) has been extensively studied due to their

13   harmful effects to health and environment. In this work, Encapsulated Ionic Liquids

14   (ENILs) are used as catalysts for the NO oxidation at humid conditions and low

15   temperatures. Hollow carbon capsules (C$_{Cap}$) were first synthetized to contain different

16   amounts of 1-butyl-3-methylimidazolium nitrate IL ([bmim][NO$_3$]), responsible for the

17   catalytic oxidation. Then, the materials were characterized using different techniques, by

18   analyzing microstructure, porosity, elemental composition and thermal stability. The

19   catalytic performance of ENIL materials was tested for NO conversion at different

20   conditions. Thus, NO concentration was fixed at 2,000 ppm at dry and humid conditions.

21   Then, the methanol promotion of the reaction was demonstrated, increasing the NO

22   conversion values in all cases, and the alcohol/water ratio was optimized. The temperature

23   effect was studied as well, using the optimal conditions based on the previous

24   measurements. The results reflect that humid conditions do not have a negative effect in

25   terms of NO conversion when using ENILs, opposite behavior as the observed for C$_{Cap}$

26   and traditional catalysts studied before. Low amount of IL inside the material (40% in

27   mass) was found to be the optimum for the task, reaching conversions of almost 45% in

28   near industrial conditions of temperature and O$_2$ and H$_2$O concentrations in the flue gas

29   with a GHSV = 10,000 h^{-1}.

1

Introduction

Nitrogen oxides (NO_x) are one of the major air pollutants from traditional electrical production as fossil fuel combustion, leading to well-known harmful effects [1,2]. These negative effects comprise not only to the human health, causing important respiratory problems [3], but also atmospheric pollution by acid rain, photochemical smog and ozone layer depletion [4,5]. The major constituents of NO_x are nitrogen dioxide (NO_2) and nitric oxide (NO), which is an intermediate of the nitric acid synthesis in the chemical industry. Due to the low solubility of this gas in traditional solvents [6], it is attractive to develop systems to remove or convert this compound into value-added or not harmful products. The most important technologies of the chemical industry to remove NO_x present in the flue gas are the well stablished SCR (selective catalytic reduction) and SNCR (selective non-catalytic reduction) of NO_x [7,8]. However, these methods are not able to remove NO_x completely because of some disadvantages during their use at high operating temperatures [9], which also means high costs of the process. The catalysts typically used in SCR, mainly based on V_2O_5, work at temperatures above 300 ºC [10], taking advantage of the high temperatures of the power plants systems but placed in high dust position, promoting catalyst deactivation. However, other industrial units like waste incineration plants and ships demand also low temperature –end-of-pipe- de-NO_x technologies. Therefore, research efforts have been centered on the development of new catalysts able to eliminate NO at lower temperatures. In this sense, not only the reduction process was taken into account, but others such as catalytic oxidation that was proved to work at lower temperature.

Several works were published in this field using zeolites [11] or carbonaceous materials [12] in presence of water at low temperature, giving as conclusion that the reaction occurs in the micropores of the material. Recently, an interesting work published by Ghafari *et al.* reports conversions up to 35 % of NO to NO_2 in presence of water by using a polymer based catalyst at near room temperatures [13]. However, the presence of water decreased the polymer based catalysts performance. For this reason, it is important to develop catalysts are less affected in presence of water, or even with water as promoter to convert NO to value-added products.

Other alternatives to remove NO were also investigated, such as absorption [14,15]. In this case, the absorption capacity of NO in aqueous solutions is reported to be low [15]. For these reasons, big efforts has been tried to enhancing this absorption capacity by means

2

63 of using additives [16]. Furthermore, it was detected the easy combination of NO with

64 transition metals, so different metals were specifically designed for NO capture [17]. All

65 these absorbents were aqueous solutions, limited by the low NO solubility in water [18].

66   In last years, ionic liquids (ILs) are proposed as new chemical solvents, attracting a

67 huge number of studies in e.g. gas capture applications [19], due to their characteristic

68 properties such as high absorption capacity, low vapor pressure and high thermal and

69 chemical stability [20], among others. Therefore, ILs have been extensively evaluated in gas

70 capture, for instance of CO_2 [21], SO_2 [22], H_2S [23], NH_3 [24], and volatile organic compounds [25].

71 It is remarkable that, however, few works on NO capture by ILs have been reported so

72 far. Chen *et al.* [26] reported the first functional IL to capture NO, with the disadvantage of

73 the high difficulty in the synthesis stage. Then, Sun *et al.* [27] synthetized a metallic

74 functional ionic liquid able to chemically absorb NO. Recently, Kunov-Kruse *et al.* [28]

75 reported that the IL 1-butyl-3-methylimidazolium nitrate ([bmim][NO_3]) is a successful

76 catalyst for NO oxidation into nitric acid in presence of water. However, it is well stated

77 that the practical application of ILs are limited by their unfavorable transport properties

78 [29, 30]. In fact, several efforts have been centered on developing systems and materials able

79 to reduce the kinetic control in the absorption operations based on ILs [31-33]. Thus,

80 Supported Ionic Liquid Phase (SILP) concept was invented [34-36]. It consists of IL

81 deposition in the pores of a solid support (silica, carbon, among others). In the case of gas

82 capture application, these materials increase the mass transport rates compared with pure

83 ILs due to the increase in the gas-liquid interfaces [37]. In the case of catalysis, it can be

84 used like a solid heterogeneous catalyst for continuous fixed bed reactor systems [35, 38].

85 Recently, SILPs have been applied to different catalytic reactions. An efficient catalytic

86 system based on metal ligand free in an environmental friendly IL system was

87 successfully developed for Suzuki cross-coupling reactions [39]. Another metal/IL

88 supported on nano-silica based catalysts were employed in the aldehyde C-H activation

89 showing excellent yields of the desired aryl ketones [40]. Catalysts based on copper-doped

90 silica supporting acidic ILs (based on [HSO_4]$^-$ anion) demonstrated a good performance

91 on Biginelly reaction [41]. In last years, CO_2 valorization has attracted the attention of the

92 scientific community, using SILPs as catalysts for the reaction of cycloaddition of

93 epoxides [42, 43]. Regarding NO separation, the first approach using SILP materials (silica

94 as support) was successfully applied by Fehrmann's group [33]. However, the IL loading

95 can limit the practical application of gas capture [32]. A more recent alternative has

96   emerged: the Encapsulated Ionic Liquids (ENILs) concept, in which a high amount of IL

97   (up to 80%) is contained inside hollow carbon capsules (internal diameter of 400-700 nm)

98   with high specific surface area [31]. The performance of ENIL materials was tested by

99   different gas capture applications such as ammonia [31, 44] and CO_2 in both physical [30, 45]

100   and chemical [46-48] absorption. These works concluded that the encapsulation of the IL

101   does not decrease absorption capacities and increase very significantly the absorption

102   rates, due to the strong increase of contact surface after IL encapsulation. Furthermore,

103   the nature of the IL does not significantly matter to the gas capture kinetics when using

104   ENIL materials, since it is controlled by carbon capsule morphology [48]. Therefore,

105   ENIL materials are able to solve the kinetic restrictions that pure ILs present in gas

106   capture applications.

107   At this point, it emerged the idea of taking advantage of the improved mass transfer

108   kinetics of ENIL materials for its application in NO oxidation by ionic liquid catalysis.

109   Therefore, we propose 1-butyl-3-methylimidazolium nitrate ([bmim][NO_3]) for its

110   encapsulation into ENIL materials with different loadings. The IL selection was decided

111   based on the previous work in which it was demonstrated that could be NO oxidized. The

112   aim of this work is to evaluate the performance of a new support (based on hollow carbon

113   capsules) in which the IL is encapsulated forming the ENIL materials in NO catalytic

114   oxidation into NO_2, HNO_2 and HNO_3 in presence of water at low temperatures.

Experimental section

115   *Materials*

117   The IL 1-butyl-3-methylimidazolium nitrate (98 %) was purchased from Iolitec.

118   The reagents used for hollow carbon capsules synthesis: phenol (99 %),

119   paraformaldehyde (95-100 %), aluminum trichloride (95-100 %), ammonia (34 %) and

120   absolute ethanol were supplied by Panreac. In addition, tetraethylorthosilicate (98 %)

121   (TEOS), hexadecyltrimethoxysilane (90 %) (C16TMS) and hydrofluoric acid (48 %)

122   were supplied by Sigma-Aldrich. Nitrogen, air and the mixture containing 10,000 ppmv

123   of NO in nitrogen were supplied by AGA. The methanol (99.8 %) used for the promoted

124   NO oxidation was supplied by Sigma-Aldrich.

125   *ENIL synthesis*

126   The hollow carbon capsules (C_{Cap}) were synthetized as ENIL materials following

127   the procedure reported by Büchel *et al.* [49]. This methodology has been successfully

128 applied by our group in the last years [46, 48, 50, 51] to obtain the C_{Cap} and then the ENIL

129 materials for their use in gas capture applications. The full description of the procedure

130 can be found in the referred works. In summary, C_{Cap} were synthetized following a

131 "templating" method in which the solid core and the mesoporous shell aluminosilicate

132 (SCMS) were used as template. The colloidal solution was maintained at 30 ºC with

133 vigorous stirring to achieve homogenous diameters of the spheres. Then, the shell was

134 grown around the silica core by adding TEOS and C16TMS (to give porosity to the double

135 shell). After being filtrated and calcined at 550 ºC, the SCMS was impregnated by a

136 phenolic resin (generated in situ) that will serve as carbon precursor (prior pyrolysis

137 stage). To accomplish this, aluminum trichloride was impregnated in the SCMS as

138 catalyst of the phenolic resin generation. Then, a mixture of paraformaldehyde and phenol

139 was added to completely impregnate the material generating the phenol-

140 paraformaldehyde resin. The resulting material could be heated until 160 ºC that is the

141 curing temperature of the resin, during 5 hours and then increased until 850 ºC under a

142 nitrogen atmosphere to accomplish the pyrolysis of the material. The resulting carbon

143 was washed with HF in order to remove the remaining silica present, being able to obtain

144 the final hollow carbon capsules (C_{Cap}).

145   From C_{Cap}, the ENIL materials were prepared using incipient wetness impregnation.

146 400 mg of C_{Cap} were used and 1 mL of methanol-IL solution was added drop by drop

147 onto the carbon support. Then, the resulting ENIL materials were heated until 85 ºC to

148 completely remove the remaining methanol. In this work, four different ILs loadings were

149 tested (20, 40, 60, and 80 % w/w). The complete synthesis process is shown in Scheme 1.

150 The methodology used was applied in several works of our group demonstrating the

151 homogenous distribution of the IL inside the C_{Cap} [30, 44, 46-48].
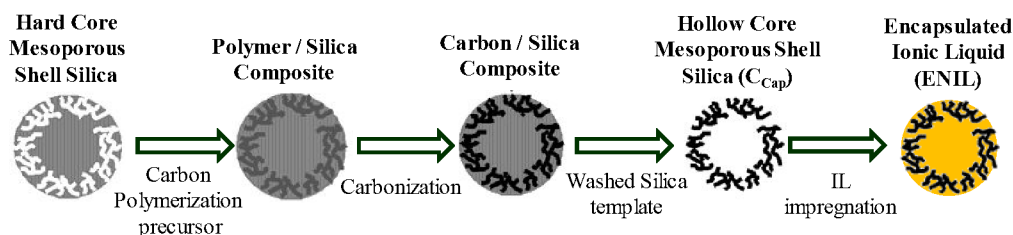
152   Scheme 1: ENIL synthesis scheme

153 *ENIL characterization*

154   The C_{Cap} samples were characterized by means of elemental analysis in a LECO

155 CHNS-932 apparatus. The porous structure of the hollow spheres and ENIL materials

5

156   was also characterized by 77 K N_2 adsorption/desorption using a TriStar II 3020

157   (Micromeritics) equipment after 10 h of degassing at 0.1 mbar and 393 K. The pore size

158   distribution was calculated using t method. The microstructure and morphology of C_{Cap}

159   were studied by transmission electron microscopy (TEM) using a JEOL JEM 2100 HT

160   microscope. Then, the ENIL materials prepared were characterized by means of thermal

161   gravimetric analysis (TGA) and elemental composition to check the amount of IL inside

162   the material before and after reaction using a Mettler Toledo TGA/DSC 1 STARe system.

163   This was carried out under a N_2 flow of 50 mL/min from room temperature until 600 ºC

164   with a heating rate of 10 ºC/min.

165   *NO oxidation measurements*

166   The prepared ENIL materials and hollow carbon spheres (C_{Cap}) were tested as NO

167   catalysts using a fixed-bed reactor with ENILs volume of approximately 1.2 cm^3,

168   corresponding to masses between 0.4-1.0 g depending on the load of IL used. Most

169   experiments were carried out at room temperature (near 24 ºC). However, in the

170   experiments in which the temperature was changed, the reactor was placed inside an oven

171   able to control the temperature (regeneration experiments as well). A flue gas was passed

172   through the reactor with a NO concentration of 2,000 ppm. The O_2 content was varied

173   from 6.2 to 16.8 % and balanced with N_2. Three mass flow controllers were used: i)

174   connected to a 1% $NO-N_2$ bottle; ii) connected to an air bottle; iii) connected to a N_2

175   bottle. The total gas flow for each experiment was set at 200 mL/min. All the reactions

176   were conducted at atmospheric pressure. Furthermore, the top of the reactor was fitted

177   with a three-way valve that allows introducing the gases and the liquid inside the fixed-

178   bed reactor. The flow of the liquid was controlled by a NE-300 Syringe Pump. In this

179   sense, the relative humidity (RH) of the flue gas was changed and studied from 10 to 75

180   % utilizing a syringe filled of deionized water. The addition of the methanol to promote

181   the oxidation reaction was accomplished by adding a water/methanol solution to the

182   system by the Syringe Pump. The methanol concentration (varied from 100 to 1600 ppm)

183   and the flow rate needed were calculated in each experiment in order to maintain the

184   desired conditions. The bottom of the reactor was conducted into a gas cuvette inside a

185   Thermo Scientific Evolution 220 UV-Visible Spectrophotometer. Each measurement

186   collects the whole spectrum from 200 to 600 nm. NO have absorption bands in the ultra-

187   violet (UV) region at 204 nm, 215 nm and 226 nm. This last peak was used to quantify

188   the NO in the exit of the reactor and calculate the conversion. Peakfit.m matlab script was

6

189   used for deconvolution of the three peaks, using last one at 226 nm to calculate

190   conversions as a function of the peak area using a standard curve performed with different

191   NO concentrations mixed with an inert gas (N_2). Other peaks that could be identified in

192   the spectra are due to NO_2 having a broad peak around 405 nm and HNO_2 that presents

193   four different peaks from 340 to 390 nm; and the HNO_3 exhibiting a broad peak in the

194   NO region (from 200 to 250 nm). These peaks can indicate which species are being

195   formed depending on the operation conditions tested. In all cases, the conversion was

196   calculated at steady state, i.e. identical spectra obtained during at least 2 hours. Before

197   changing the relative humidity of the inlet gas, the desorption experiment was carried out

198   after heating the sample up to 130 °C using 100 mL/min of N_2 in presence of water (ratio

199   1:1) to totally remove the water, methanol and nitric acid present in the sample.

Results

201   *C_{Cap} and ENILs characterization*

202   The hollow carbon capsules (C_{Cap}) and the four prepared ENIL materials were

203   characterized by means of microscopy, pore structure, elemental analysis and thermal

204   stability. Thus, Figure 1A shows TEM microscopy image of the C_{cap} while Figure 1C

205   shows the size distribution of the analyzed sample by several TEM images. Figure 1B

206   presents the N_2 adsorption-desorption isotherm of the C_{Cap} before the incorporation of

207   [bmim][NO_3] IL.
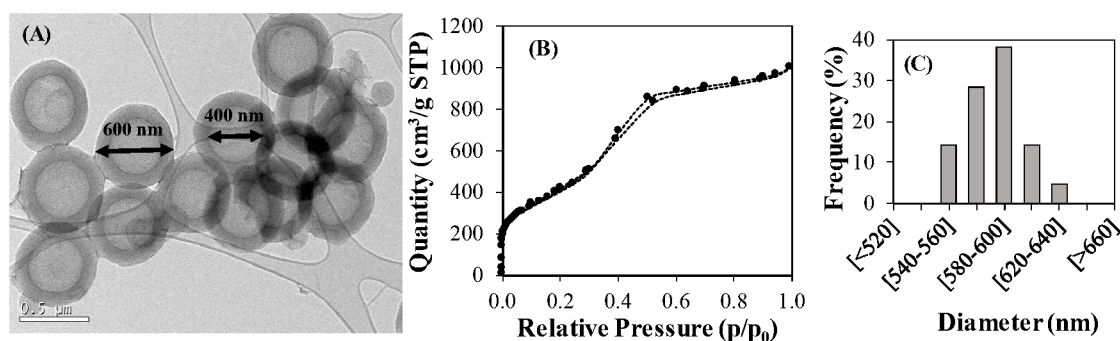
208   Figure 1: **(A)** TEM image of the hollow carbon capsules (C_{Cap}) to prepare ENIL materials;

209   **(B)** N_2 adsorption/desorption isotherms @ 77 K of C_{Cap} and **(C)** size distribution of C_{Cap}

210   Figure 1A shows the homogenous size distribution of the material with spherical

211   shape and an external diameter of almost 600 nm with a shell thickness of 200 nm and a

212   large central hole. The N_2 adsorption-desorption isotherm (Figure 1B) is typical of a

213   mesoporous material with a significant microporosity contribution (both as a consequence

7

214   of the porosity of the shell). Table 1 reflects the elemental analysis and the summarized

215   information extracted from the N$_2$ adsorption-desorption isotherms.

216

217   Table 1: Carbon capsules (C$_{Cap}$) characterization by means of elemental analysis and N$_2$
218   adsorption-desorption @ 77 K.

Characterization technique			
Elemental Analysis		N$_2$ adsorption-desorption	
% C (w)	91.40	S$_{BET}$ (m^2/g)	1,494
% H (w)	1.80	V$_{micropore}$ (cm^3/g)	0.55
% N (w)	0.10	V$_{mesopore}$ (cm^3/g)	0.68
		Pore size (Å)	41.35

219

220   The elemental analysis extracted from Table 1 confirm the carbonaceous nature of

221   the material (more than 90% of carbon). The incorporation of the different amounts of IL

222   in the support is possible due to the high porosity. The material possesses both

223   mesoporosity and microporosity mainly based on the porous shell grown around the

224   central hollow core. Thus, the average pore size is almost 40 Å, which reflects the

225   mesoporosity of the material. In that way, the different amounts of IL can be incorporated

226   in the support filling the double shell first (until 40% of IL) and the large central hole

227   afterwards [31]. Once the C$_{Cap}$ was synthetized and characterized, the ENIL materials can

228   be prepared with different amounts of IL. In order to check the amount of IL incorporated

229   in each sample, Figure 2 shows the TGA analysis of each one.
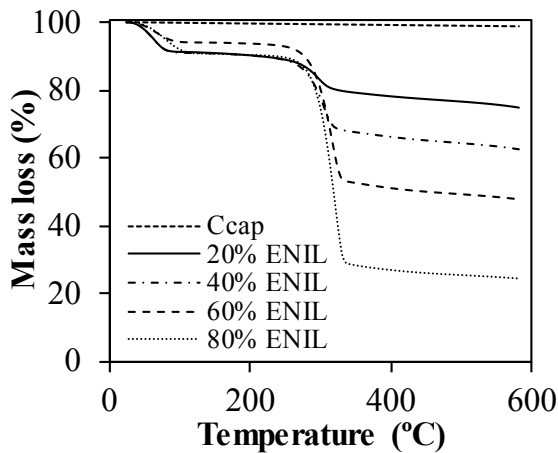

230   Figure 2: TGA analysis of the materials used in this work: hollow carbon capsules (C$_{cap}$)
231   and ENIL materials with four different IL loading (20, 40, 60 and 80 % of [bmim][NO$_3$]).
232   Analysis carried out with a temperature increase of 10 °C·min^{-1} under 50 mL·min^{-1} of N$_2$.

8

233   Starting with the TGA analysis of C_{Cap}, as can be seen in Figure *2*, our support is

234   stable at least until 600 °C under nitrogen. Therefore, using this curve as reference, it is

235   possible to estimate the amount of IL present in each sample taking into account the

236   remaining mass at 600 °C (attributed to the carbon support). In all cases, after a little

237   decay prior to 100 °C (possible sorbed water) the final value corresponds perfectly to the

238   nominal amount of each material. The elemental composition results of each material (see

239   Table S1 of Supplementary Information) confirm the conclusions of TGA analysis. In

240   addition, the pore size distribution of all the ENIL materials are shown on Figure S1 of

241   the Supplementary Information confirming almost the same average pore size (40 Å) but

242   decreasing the pore volume by increasing the IL load on ENILs. The experimental N_2

243   adsorption/desorption isotherms are also included in Figure S2 of Supplementary

244   Information. An increase in the IL loading inside ENIL material leads to the filling of the

245   pores until 60-80%, in which all remained completely occupied or blocked by IL [31, 32].

246   *NO oxidation in dry conditions*

247   The different prepared catalysts were first tested in absence of moisture. Prior to

248   test the ENIL materials performance in NO catalytic oxidation, it is important to

249   understand the behavior of the support (C_{Cap}) under different oxidation conditions. Figure

250   3 shows the NO conversion in the hollow carbon capsules using different O_2 contents. In

251   this case, the reaction involved in experiments in dry oxygen condition is depicted in

252   Eq. 1.

253         $NO + ½ O_2 \rightarrow NO_2$ (1)

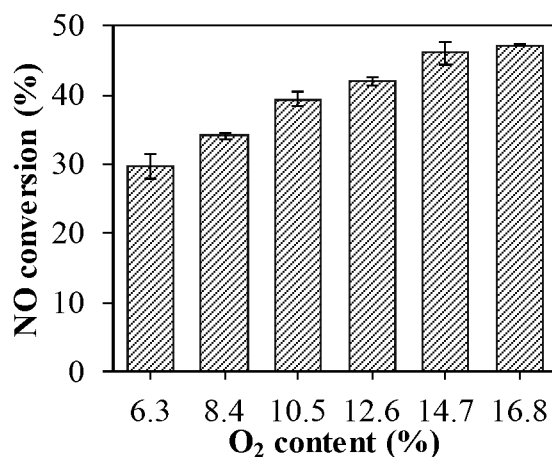254   Figure 3: NO conversion of hollow carbon capsules (C_{cap}) in dry conditions at different
255   oxygen contents. Gas composition: 2,000 ppm NO, 6.3-16.8% O_2, balance N_2, Flow:
256   200 mL·min^{-1}, GHSV=10,000 h^{-1}. Experiments conducted at room temperature.

9

257   As can be seen, the trend clearly shows higher catalytic activity by increasing the

258   amount of O_2 in the system, reaching almost 48 % of conversion at 16.8% of O_2. This

259   means that the presence of more O_2 in the system leads to the formation of more NO_2,

260   resulting in higher conversion values (see Figure S3 in Supporting Information).

261   Compared to those previously reported in the literature, we used 10.5% O_2 (almost 40 %

262   NO conversion) which corresponds to those applied at industrial conditions to treat almost

263   2,000 ppm of NO [52]. Zeolite based catalysts exhibit NO conversions from 5 to 45 % [11]

264   depending on the modifications carried out, concluding that those with higher micropore

265   volume show the greatest performance. Zhang *et al.* [12] reported NO conversions up to 57

266   % using microporous activated carbons. Sousa *et al.* [53] used doped carbons reaching

267   conversions up to 75 % in the best case. In view of all these results, our C_{Cap} material,

268   later used as support for ENIL materials, presents NO conversion in dry O_2 conditions in

269   the range of the zeolite catalysts and slightly lower when compared with activated carbons

270   prior to their modification at almost same conditions. These differences may be attributed

271   to the different porous structure of the materials. It is believed and proved that a high

272   microporous structure leads to higher conversions. In the case of our material, it is

273   basically a mesoporous material but presenting high micropore volume (see Table 1). The

274   C_{Cap} performance can be compared with the ENIL catalysts at 10.5% of O_2. In Figure 4,
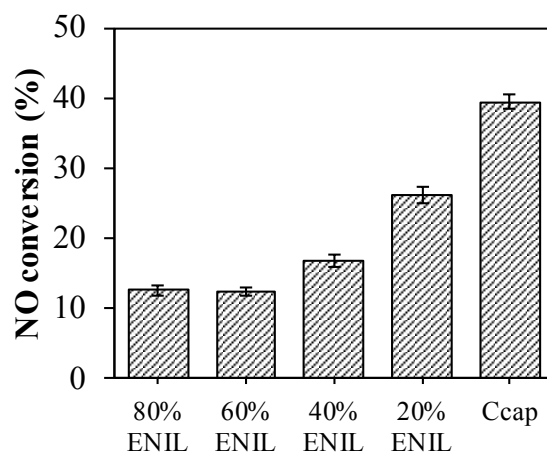
275   the NO conversion reached by each material (including the previous discussed C_{Cap}) are

276   compared.

277   Figure 4: NO conversion of the different materials of the work in dry conditions. Gas
278   composition: 2,000 ppm NO, 10.5% O_2, balance N_2, Flow: 200 mL·min^{-1},
279   GHSV=10,000 h^{-1}. Experiments conducted at room temperature.

280   As can be seen, NO conversion decreases by increasing the amount of IL in the

281   catalyst until the conversion remains constant (from 60% IL loading). This could be

10

282   explained due to filling of the pores of the C_{Cap} material (see the reduction in BET area

283   while increasing the IL loading in Table S1 of the Supplementary Information). In the

284   case of 20% and 40% ENIL material, the higher conversion may be attributed to partly

285   filled pores exhibiting more efficient IL distribution on the pore surface. From the

286   previous reported data with [bmim][NO$_3$] IL [28], it seems that the presence of water is key

287   leading to the formation of more [NO$_3$]$^-$ anions (anion part of the IL) that may improve

288   the NO removal.

289   *NO oxidation in wet gas*

290   In order to simulate near industrial conditions the catalytic performance of our

291   materials was investigated in gas streams that contain around 10% O$_2$ and water.

292   Experiments in wet conditions follow the reaction of Eq. 2. More details about the

293   mechanism of NO oxidation reaction in presence of water using [bmim][NO$_3$] can be

294   found in previous works [28, 54].

295            $$4 \, NO + 3 \, O_2 + 2 \, H_2O \rightarrow 4 \, HNO_3 \qquad\qquad (2)$$
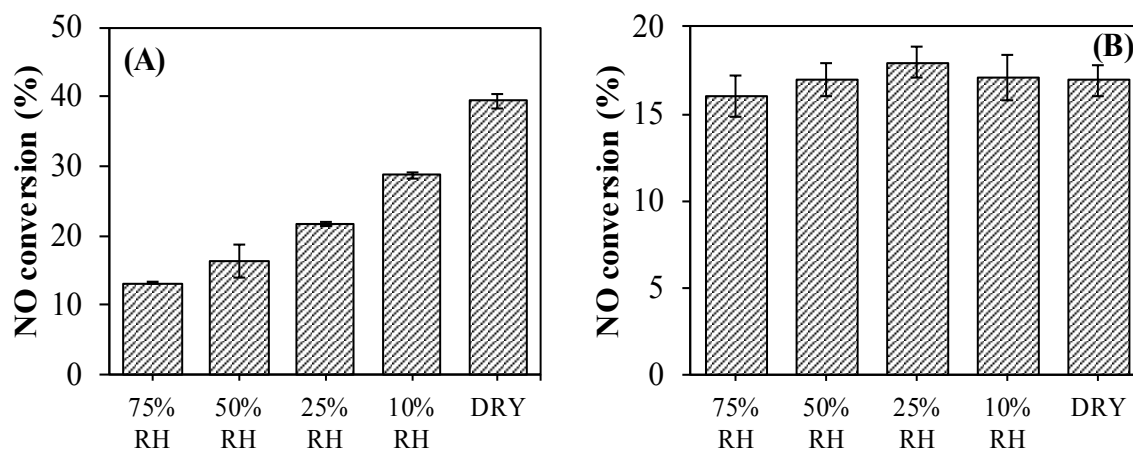
296   Figure 5: NO conversion of **(A)** the hollow carbon capsules (C$_{cap}$) and **(B)** the 40 %
297   [bmim][NO$_3$] ENIL material in different dry and wet conditions (from 10 to 75% Relative
298   Humidity). Gas composition: 2,000 ppm NO, 10.5% O$_2$, balance N$_2$, Flow: 200 mL·min^{-1},
299   GHSV=10,000 h^{-1}. Experiments conducted at room temperature.

300   Figure 5A clearly shows the catalytic inhibition when water was added into the

301   system employing C_{Cap} as catalyst. NO conversion reaches only a value of 13% at 75%

302   RH. This may be explained by the decrease of the NO adsorption mainly caused by the

303   competitive water adsorption. Some works reported that water affects negatively the NO

304   oxidation using activated carbons (AC) or zeolites. They reached the same conclusion:

305   the NO oxidation inhibition in presence of water is caused by adsorption competition.

11

306   Thus, Mochida *et al.* [55] showed a huge decrease in conversion by increasing RH in AC

307   catalysts. Another work by Mochida *et al.* [56] showed the limitation of RH > 60% to the

308   NO oxidation using AC catalysts. Guo *et al.* [57] reported the complete stop in NO oxidation

309   when RH is higher than 20% using AC catalysts. The moisture influence was also studied

310   in zeolite based catalysts [58] reaching conversions of only 10% when 8% of H_2O is present

311   in the flue gas stream, showing a dramatic inhibiting effect in that kind of catalysts. The

312   most recent study at wet conditions concerns a new polymer based catalyst [13] in which

313   the inhibition was also demonstrated when 50% RH was employed. In addition, we

314   believe that the inhibition may also be caused by means of *capillary condensation*,

315   described by the Kelvin equation [59]. At the pore diameter of C_{Cap} (about 41 Å, see Table

316   1), *capillary condensation* at room temperature is expected to occur at a RH around 50-

317   60% [60] and may thus cause the observed deactivation in Figure 5A for RH > 50%. This

318   phenomenon definitely does not occur when the IL is completely filling the pores of the

319   support. As can be seen, the presence of water does not inhibit the NO oxidation when

320   using ENIL material. This may be explained by the different NO oxidation mechanism

321   by the [bmim][NO_3] catalyst in presence of water that leads to conversion to HNO_3

322   instead of NO_2 in the dry gas as concluded in the previous work [28]. A slight increase in

323   the HNO_3 and decrease in the NO_2 regions of the UV-Vis spectrum (see Figure S2 in

324   Supporting Information) was thus found by adding water to the system compared to the

325   C_{Cap} catalyst. Therefore, this IL catalyst the first reported NO oxidation catalyst that is

326   not negatively affected by presence of water.

327   Figure 6 shows the NO conversion of the studied materials at two different gas
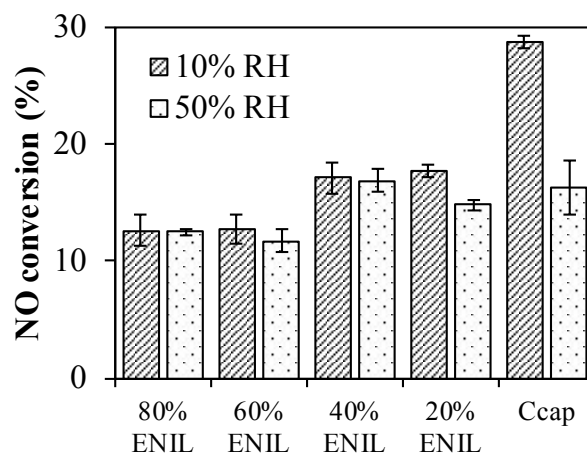
328   humidity levels.

329   Figure 6: NO conversion of the different materials at two different wet conditions (10 and
330   50% Relative Humidity). Gas composition: 2,000 ppm NO, 10.5% O_2, balance N_2, Flow:
331   200 mL·min^{-1}, GHSV=10,000 h^{-1}. Experiments conducted at room temperature.

332   For 10% RH, it can be seen that the C_{Cap} material exhibits the highest conversion
333   compared to the ENILs. It seems therefore the water levels are not enough for the ENIL
334   materials to exhibit a decreased performance. The conversion follows almost the same
335   trend as observed for the dry experiments, i.e. the NO conversion decreases while
336   increasing the amount of IL in the material until 60% loading above, which it remains
337   constant. However, a closer look reveals that the presence of water in the gas for the 20%
338   ENIL catalyst seems to be partially inhibited compared to dry conditions, as in the case
339   for the C_{Cap}. This may mean that there are still some pores not completely filled with the
340   IL.

341   Analyzing the 50% RH exposure, the presence of available pores for NO oxidation
342   in the case of 20% ENIL material seems obvious due to the observed reduction in the NO
343   conversion (but to a lesser extent than for C_{Cap}) when compared with 10% RH exposure.
344   This behavior was also concluded in terms of available pores while increasing the amount
345   of ILs in the support by Lemus *et al.* [31, 32]. The rest of the materials exhibit unaltered
346   behavior, since their activities are not affected by the addition of more water. If we now
347   compare the performance of the materials at 50% RH, it can be seen that the 40% ENIL
348   exhibits slightly higher NO conversion than C_{Cap}, probably due to the difference in
349   mechanism, while the 20% ENIL material shows almost the same behavior as C_{Cap},
350   followed closely by the other two ENILs. Thus, it can be concluded that flue gas streams
351   that contain high amount of water does not affect the ENIL materials performance (in
352   terms of NO conversion), in contrast to the typical carbon materials (C_{Cap}), in which the
353   reaction is strongly inhibited.

354   *Methanol promoted NO oxidation in wet gas*

355   In the 1990's, methanol promoted NO oxidation at high temperatures (from 700 ºC
356   up to 1,000 ºC) was investigated [61, 62]. An increase in terms of NO conversion was
357   reported when methanol was added to the system. Zamansky *et al.* proposed [62] the
358   addition of a MeOH/H_2O_2 mixture to further increase the catalytic performance. No more
359   work related to the methanol promoted NO oxidation has been published as far as we
360   know. Then, research efforts moved to methanol oxidation in presence of NO. Thus, some
361   papers [63-65] showed an increase in the MeOH conversion in presence of NO (temperatures

13

362   from 600 up to 1,200 ºC). Furthermore, they proposed a possible mechanism of the

363   oxidation reaction, concluding that radical formation in presence of NO was occurring.

364   Since methanol promotes the NO oxidation, we screened different methanol

365   concentrations to examine our catalysts performance. As far as we know, this is the first

366   work in which this methodology is applied at room temperature using IL-based catalysts.

367   Thus, Figure 7 shows the NO conversion as a function of the RH and the methanol

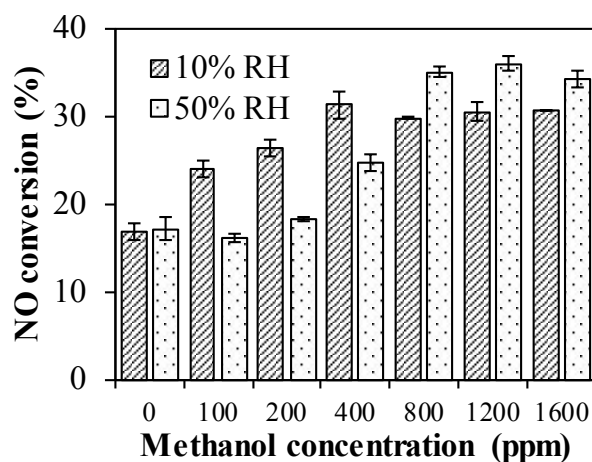368   concentration for the 40% ENIL material.

369

370   Figure 7: NO conversion in 40% [bmim][NO$_3$] ENIL material with relative
371   humidity of 10 and 50% and different concentrations of MeOH in the gas phase. Gas
372   composition: 2,000 ppm NO, 10.5% O$_2$, balance N$_2$, Flow: 200 mL·min^{-1}, GHSV=10,000
373   h^{-1}. Experiments conducted at room temperature.

374   From Figure 7, it can be seen how the NO conversion increases by increasing the

375   methanol concentration until reaching a maximum. That maximum depends on the RH

376   studied but it is located at a MeOH/NO ratio between 0.2-0.4 depending on the RH.

377   Starting with 10% RH, it is clearly seen that NO conversion increases while increasing

378   the amount of methanol until 400 ppm of MeOH whereafter it remains constant up to

379   1,600 ppm of MeOH. For 50% RH, the same trend is observed but the maximum is

380   reached at 800 ppm of MeOH. It seems that for 50% RH, the NO conversion is higher

381   than at 10% RH at methanol concentrations above 800 ppm. This interesting difference

382   in the trends might be explained by increased HNO$_3$ formation when more water is

383   present in the system (see figure S4 of the Supporting Information). An interesting work

384   by Xiao et al. [66] studying the mechanism of the methanol oxidation in presence of NO

385   (room temperature performed as well) indicated that NO$_2$ may play a role in the methanol

386   oxidation. They proposed a series of intermediate reactions involved in the MeOH

14

387   oxidation when NO_2 is present. In this context, we believe that two of the proposed

388   reactions may be occurring in our system:

389            $CH_3OH + \cdot NO_2 \rightarrow \cdot CH_2OH + HONO$ (3)

390            $CH_3OH + \cdot NO_2 \rightarrow CH_3O \cdot + HONO$ (4)
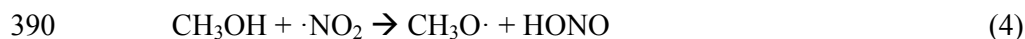
391   Reactions (3) and (4) may be occurring in our system due to the observed nitrous

392   acid (HONO) and the absence of NO_2 in the UV-Vis spectrum (see Figure S5 in

393   Supporting Information), not only while adding the first droplets but also at the steady

394   state (especially when high conversions were found). This was immediately found when

395   methanol was added to the system. Furthermore, huge amounts of HNO_3 were detected

396   while adding MeOH to the system (see Figure S5 in Supporting Information), this may

397   be explained by the proposed mechanism by Kunov-Kruse *et al.* [28] when using

398   [bmim][NO_3] as catalyst in which HNO_3 was formed in the catalytic reaction in presence

399   of water. In addition, the presence of HONO may lead to fast formation of HNO_3 (due to

400   nitrous acids well-known instability). Therefore, promoted oxidation of NO in presence

401   of MeOH may be explained by radical formation in both the liquid and the gas phase.

402   Low amounts of MeOH that remain absorbed on the IL are simply removed by heating

403   up the sample to 130 ºC. This compound can be easily separated from the others involved

404   in the reaction due to the high differences in their volatilities. Future works will be

405   centered on the study of the mechanism of reaction, getting attention the possible other

406   value-added products formed during the reaction.

407   Based on the optimized MeOH addition, two different concentrations for each RH

408   (200 and 400 ppm for 10% RH and 400 and 800 ppm for 50% RH) respectively were

409   selected for testing the different materials.

410

15

Figure 8: NO conversion of the different materials at relative humidity of **(A)** 10% RH
412   and **(B)** 50% RH and two different concentrations of MeOH in the gas phase. Gas
413   composition: 2,000 ppm NO, 10.5% O_2, balance N_2, Flow: 200 mL·min^{-1},
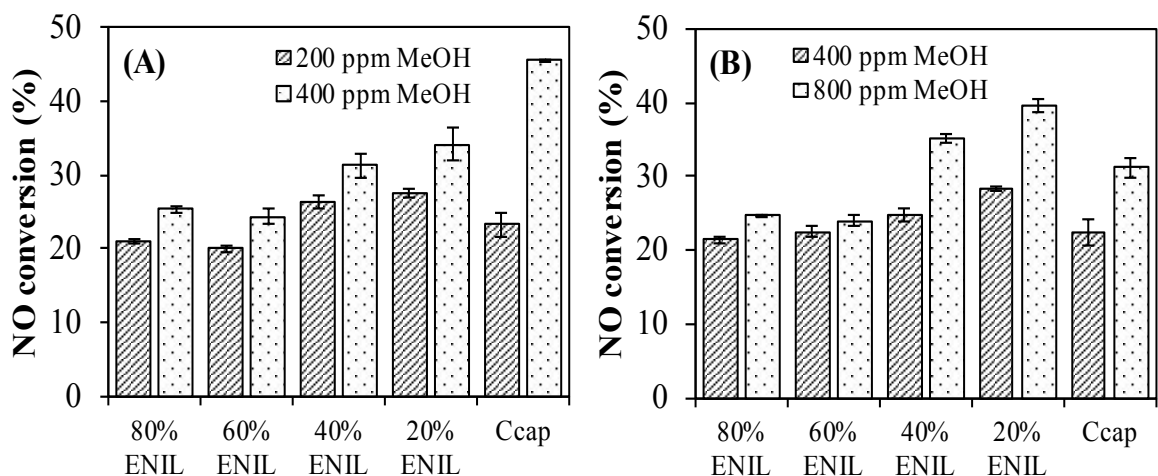414   GHSV=10,000 h^{-1}. Experiments conducted at room temperature.

415   In

416   Figure 8A, the methanol promoted NO conversions of the different materials at 10%

417   RH can be analyzed. In general terms, all the materials exhibit greater conversions with

418   the addition of MeOH when compared to the same moisture conditions without MeOH.

419   For 200 ppm methanol, it can be seen that the 20% ENIL material presents the highest

420   NO conversions while it seems that the amount of MeOH added is not enough for

421   overcoming the inhibition in C_{Cap} material pores. However, when increasing to 400 ppm

422   of MeOH, the hollow carbon capsules exhibit the highest activity. The measurements

423   show in general that the addition of methanol promotes the reaction at wet conditions

424   independent of the catalyst used.

425

426   Figure 8B shows that the 20% and 40% ENIL materials present the highest

427   conversion at 50% RH, even higher than hollow carbon capsules. This suggests that at

428   high concentrations of water, the presence of MeOH is not compensating for the

429   inhibition of the NO reaction in the C_{Cap} material probably due to pore condensation of

430   water. The results confirm that for wet conditions with addition of methanol, the ENIL

431   materials exhibit a positive effect regarding the NO removal (increase of more than 50%

432   in NO conversion when compared to the same moisture conditions without methanol -

433   Figure 6).

16

434   It is important to remark that after testing the performance of each material, TGA

435   analysis was performed to check the amount of IL that remains in the support (see Figure

436   S6 in Supporting Information) after adding water and methanol to the system. In all cases,

437   it was obtained that the same initial amount of IL remained inside the support compared

438   to before the catalytic tests.

439   Table 2: NO oxidation performance of different catalysts for dry and wet conditions

Catalyst	NO dry conversion (%)	NO wet conversion (%)	Ref.
Active carbon	69	0	[57]
Active carbon	94	0	[57]
Active carbon nanofibers	73	18	[55]
Active carbon nanofibers	64	16	[55]
Active carbon fibers	89	15	[56]
Porous polymers	43	35	[13]
Porous polymers	48	31	[13]

440

441   Table 2 summarizes NO conversion results previously reported in the literature in

442   dry and wet conditions. The experimental conditions are close to those used in our work.

443   As shown, catalysts based on active carbon present a practically complete inhibition when

444   water is added to the system. On the contrary, catalysts based on porous polymers were

445   reported as first materials able to oxidize NO in wet conditions, reaching a NO conversion

446   of 35%. The difference between ENIL materials and those previously reported is that they

447   are not inhibited when water is present in the system, obtaining almost the same NO

448   conversion independently of the amount of water. In fact, 40% NO conversion is the

449   maximum reached for 20% ENIL catalysts in wet conditions. Therefore, it can be

450   concluded that ENIL materials may be an alternative for catalysts typically studied on the

451   literature.

452   *Temperature effect on NO conversion*

453   Previous studies reported an increased NO conversion when decreasing the

454   temperature (a negative apparent activation energy) [67, 68], in good agreement with

455   homogenous phase oxidation [67]. Figure 9 shows the NO conversion as a function of the

456   temperature for the C_{Cap} material and the ENIL materials at 50% RH and 800 ppm of

457   MeOH.

17
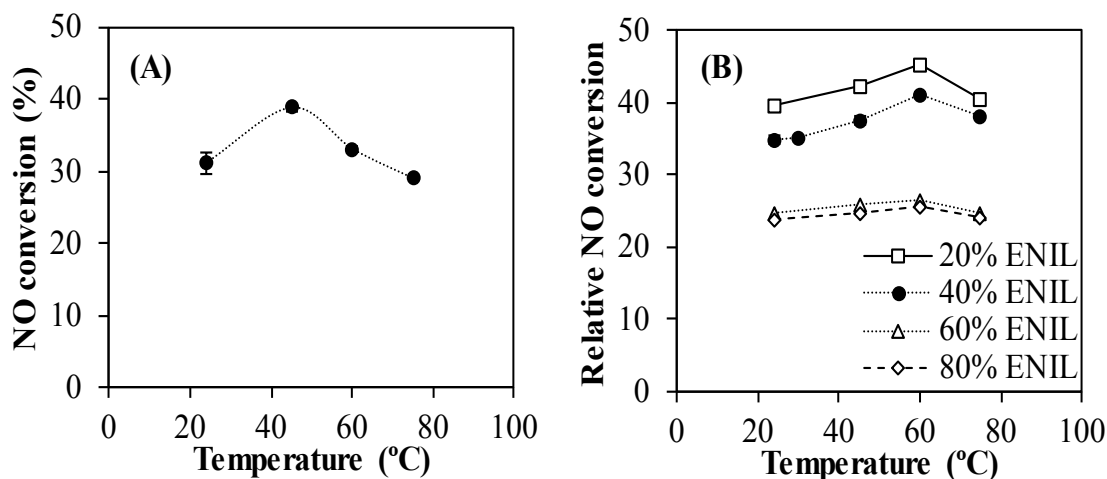
458 Figure 9: NO conversions in **(A)** hollow carbon capsules (C_{cap}) and **(B)** ENIL materials
459 as a function of the temperature using 50% Relative Humidity and 800 ppm of MeOH in
460 the gas phase. Gas composition: 2,000 ppm NO, 10.5% O_2, balance N_2, Flow: 200
461 mL·min^{-1}, GHSV=10,000 h^{-1}.

462   As shown in Figure 9A, the C_{Cap} material optimum was found at 45 ºC while in the

463 case of the ENIL material (Figure 9B), the maximum is located at 60 ºC. In the case of

464 the ENIL material, the maximum at 60 ºC may be attributed to the competing limitations

465 (radical formation) at low temperature and the lower gas solubility in the IL at higher

466 temperatures. These conclusions concern the 20 and 40% ENIL materials in which most

467 of the IL seems to be accessible to the gas, contrary to the 60 and 80% ENILs, where the

468 temperature does not affect the NO conversion. The different temperature effect observed

469 on C_{Cap} and ENIL materials may be caused by the place in which the reaction is occurring,

470 i.e pores of C_{Cap} and IL of ENIL materials. Moreover, it may be easier to retain the

471 absorbed gas on the liquid media than on pores of solid material when temperature is

472 increased. However, in general, the impact of the temperature on the NO conversion is

473 not very important, reaching about 25% at maximum.

474   It can be concluded that the oxidation at higher temperatures (approaching flue gas

475 stack temperatures) results in a slight increment of NO conversion, i.e. at temperatures

476 close to 60 ºC, the NO conversion is in the range of 45%, in presence of water in the gas
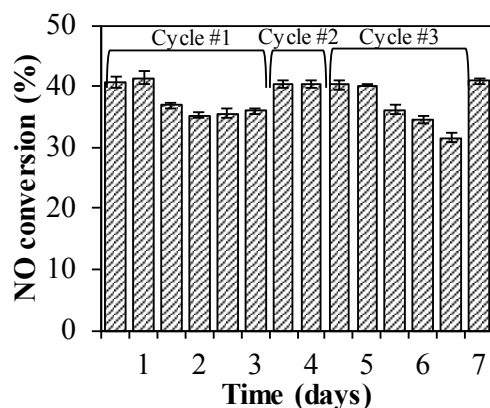
477 phase.

478

479

480

18

481

Figure 10: Stability measurements using 20% ENIL material using 50% Relative Humidity and 800 ppm of MeOH in the gas phase. Gas composition: 2,000 ppm NO, 10.5% O_2, balance N_2, Flow: 200 mL·min^{-1}, GHSV=10,000 h^{-1}.

Figure 10 presents the stability measurements of 20% ENIL material in four different cycles. As can be seen, NO conversion is maintained for 24 hours. Then, it started to decrease due to the IL saturation by NOx and HNO_3 formed. The increase in the temperature up to 130 ºC allows the complete regeneration of the catalyst reaching the same values of the fresh one. Therefore, it was demonstrated one day stability and the easy regeneration of the catalyst by a simple temperature increase.

Encapsulated Ionic Liquids (ENILs) were successfully applied as catalysts for NO oxidation at low temperatures. ENILs with different loads of the IL [bmim][NO_3] were synthetized and then characterized by means of elemental analysis, thermal stability, porous structure and microscopy. Experiments in dry gas show higher NO conversion of the hollow carbon capsules compared to ENILs, where the conversion increased with decreasing the IL loading. Experiments conducted at different relative humidities showed positive effect on NO conversion for the ENIL materials. On the contrary, the results of empty carbon material showed inhibition of the NO oxidation by increasing humidity in the system. The reaction was promoted (in presence of water) by addition of methanol to the system. The amount of methanol added to the system was optimized (at different RH), showing an optimal MeOH/NO ratio between 0.2-0.4. In this case, ENILs composed of 20 and 40% of IL exhibited the greatest performance (including hollow carbon capsules) reaching conversions near 45%. The temperature effect on the reaction revealed an optimum temperature of 60 ºC when using ENILs, accomplishing relative NO conversions 20% higher than at room temperature ones. Stability measurements revealed

19

506   NO conversion is maintained during at least 24 h without any loss. The catalyst was easily

507   regenerated by increasing the temperature up to 130 ºC. These results demonstrate

508   potential application of ENILs as catalysts at near industrial flue gas conditions to create

509   "fast SCR" for a down-stream traditional SCR catalyst.

510   **Supporting Information:** Elemental composition characterization of ENIL

511   materials involved in the work. Pore size distribution of the materials involved in the

512   work. N_2 adsorption/desorption isotherms @ 77 K of all the materials involved in the

513   work. UV-Vis Spectrum of hollow carbon capsules (C_{Cap}) in dry conditions at different

514   oxygen contents. UV-Vis Spectrum of 40% [bmim][NO_3] ENIL material (40% ENIL) in

515   dry and 10% Relative Humidity conditions. UV-Vis Spectrum of 20% [bmim][NO_3]

516   ENIL material (20% ENIL) in 50% Relative Humidity and 800 ppm of MeOH conditions.

517   TGA analysis of the materials used in this work: hollow carbon capsules (C_{Cap}) and ENIL

518   materials with four different IL loads (20, 40, 60 and 80 % of [bmim][NO_3]) after being

519   used in the catalytic reactions.

524   **References**

525   1.   Chang, S. G.; Liu, D. K., Removal of nitrogen and sulphur oxides from waste gas
526   using a phosphorus/alkali emulsion. *Nature* **1990,** *343*, 151.
527   2.   Pham, E. K.; Chang, S.-G., Removal of NO from flue gases by absorption to an
528   iron(ii) thiochelate complex and subsequent reduction to ammonia. *Nature* **1994,** *369*,
529   139.
530   3.   Kanchongkittiphon, W.; Mendell, M. J.; Gaffin, J. M.; Wang, G.; Phipatanakul,
531   W., Indoor Environmental Exposures and Exacerbation of Asthma: An Update to the
532   2000 Review by the Institute of Medicine. *Environmental Health Perspectives* **2015,** *123*
533   (1), 6-20.
534   4.   Solomon, S., Stratospheric ozone depletion: A review of concepts and history.
535   *Reviews of Geophysics* **1999,** *37* (3), 275-316.
536   5.   Volz, A.; Kley, D., Evaluation of the Montsouris series of ozone measurements
537   made in the nineteenth century. *Nature* **1988,** *332*, 240.
538   6.   Liu, N.; Lu, B.-H.; Zhang, S.-H.; Jiang, J.-L.; Cai, L.-L.; Li, W.; He, Y.,
539   Evaluation of Nitric Oxide Removal from Simulated Flue Gas by
540   Fe(II)EDTA/Fe(II)citrate Mixed Absorbents. *Energy & Fuels* **2012,** *26* (8), 4910-4916.
541   7.   Jirat, J.; Stepanek, F.; Marek, M.; Kubicek, M., Comparison of design and
542   operation strategies for temperature control during selective catalytic reduction of NOx.
543   *Chemical Engineering & Technology* **2001,** *24* (1), 35-40.

544 8.   Maisuls, S. E.; Seshan, K.; Feast, S.; Lercher, J. A., Selective catalytic reduction
545 of NOx to nitrogen over Co-Pt/ZSM-5: Part A. Characterization and kinetic studies.
546 *Applied Catalysis B: Environmental* **2001,** *29* (1), 69-81.
547 9.   Gao, Y.; Luan, T.; LÜ, T.; Cheng, K.; Xu, H., Performance of V2O5-WO3-
548 MoO3/TiO2 Catalyst for Selective Catalytic Reduction of NOx by NH3. *Chinese Journal*
549 *of Chemical Engineering* **2013,** *21* (1), 1-7.
550 10.   Busca, G.; Lietti, L.; Ramis, G.; Berti, F., Chemical and mechanistic aspects of
551 the selective catalytic reduction of NOx by ammonia over oxide catalysts: A review.
552 *Applied Catalysis B: Environmental* **1998,** *18* (1), 1-36.
553 11.   Zhang, Z.; Atkinson, J. D.; Jiang, B.; Rood, M. J.; Yan, Z., NO oxidation by
554 microporous zeolites: Isolating the impact of pore structure to predict NO conversion.
555 *Applied Catalysis B: Environmental* **2015,** *163*, 573-583.
556 12.   Zhang, Z.; Atkinson, J. D.; Jiang, B.; Rood, M. J.; Yan, Z., Nitric oxide oxidation
557 catalyzed by microporous activated carbon fiber cloth: An updated reaction mechanism.
558 *Applied Catalysis B: Environmental* **2014,** *148-149*, 573-581.
559 13.   Ghafari, M.; Atkinson, J. D., Catalytic NO Oxidation in the Presence of Moisture
560 Using Porous Polymers and Activated Carbon. *Environ Sci Technol* **2016,** *50* (10), 5189-
561 5196.
562 14.   Long, X. L.; Xin, Z. L.; Chen, M. B.; Xiao, W. D.; Yuan, W. K., Nitric oxide
563 absorption into cobalt ethylenediamine solution. *Separation and Purification Technology*
564 **2007,** *55* (2), 226-231.
565 15.   Khan, N. E.; Adewuyi, Y. G., Absorption and Oxidation of Nitric Oxide (NO) by
566 Aqueous Solutions of Sodium Persulfate in a Bubble Column Reactor. *Industrial &*
567 *Engineering Chemistry Research* **2010,** *49* (18), 8749-8760.
568 16.   Demmink, J. F.; van Gils, I. C. F.; Beenackers, A. A. C. M., Absorption of Nitric
569 Oxide into Aqueous Solutions of Ferrous Chelates Accompanied by Instantaneous
570 Reaction. *Industrial & Engineering Chemistry Research* **1997,** *36* (11), 4914-4927.
571 17.   Chien, T. W.; Hsueh, H. T.; Chu, B. Y.; Chu, H., Absorption kinetics of NO from
572 simulated flue gas using Fe(II)EDTA solutions. *Process Safety and Environmental*
573 *Protection* **2009,** *87* (5), 300-306.
574 18.   Zhu, H.-S.; Mao, Y.-P.; Chen, Y.; Long, X.-L.; Yuan, W.-K., Removal of nitric
575 oxide and sulfur dioxide from flue gases using a FeII-ethylenediamineteraacetate
576 solution. *Korean Journal of Chemical Engineering* **2013,** *30* (6), 1241-1247.
577 19.   Welton, T., Ionic liquids: a brief history. *Biophys Rev* **2018,** *10*, 691-706.
578 20.   Kosmulski, M.; Gustafsson, J.; Rosenholm, J. B., Thermal stability of low
579 temperature ionic liquids revisited. *Thermochimica Acta* **2004,** *412* (1), 47-53.
580 21.   Aghaie, M.; Rezaei, N.; Zendehboudi, S., A systematic review on CO2 capture
581 with ionic liquids: Current status and future prospects. *Renewable & Sustainable Energy*
582 *Reviews* **2018,** *96*, 502-525.
583 22.   Lin, H.; Bai, P.; Guo, X. H., Ionic Liquids for SO2 Capture: Development and
584 Progress. *Asian J. Chem.* **2014,** *26* (9), 2501-2506.
585 23.   Wang, L. Y.; Xu, Y. L.; Li, Z. D.; Wei, Y. N.; Wei, J. P., CO2/CH4 and
586 H2S/CO2 Selectivity by Ionic Liquids in Natural Gas Sweetening. *Energy & Fuels* **2018,**
587 *32* (1), 10-23.
588 24.   Bedia, J.; Palomar, J.; Gonzalez-Miquel, M.; Rodriguez, F.; Rodriguez, J. J.,
589 Screening ionic liquids as suitable ammonia absorbents on the basis of thermodynamic
590 and kinetic analysis. *Separation and Purification Technology* **2012,** *95*, 188-195.
591 25.   Bedia, J.; Ruiz, E.; de Riva, J.; Ferro, V. R.; Palomar, J.; Jose Rodriguez, J.,
592 Optimized Ionic Liquids for Toluene Absorption. *AlChE J.* **2013,** *59* (5), 1648-1656.

21

593   26.   Chen, K. H.; Shi, G. L.; Zhou, X. Y.; Li, H. R.; Wang, C. M., Highly Efficient
594   Nitric Oxide Capture by Azole-Based Ionic Liquids through Multiple-Site Absorption.
595   *Angewandte Chemie-International Edition* **2016,** *55* (46), 14362-14366.
596   27.   Sun, Y.; Ren, S.; Hou, Y.; Zhang, K.; Wu, W., Absorption of nitric oxide in
597   simulated flue gas by a metallic functional ionic liquid. *Fuel Processing Technology*
598   **2018,** *178*, 7-12.
599   28.   Kunov-Kruse, A. J.; Thomassen, P. L.; Riisager, A.; Mossin, S.; Fehrmann, R.,
600   Absorption and Oxidation of Nitrogen Oxide in Ionic Liquids. *Chemistry-a European*
601   *Journal* **2016,** *22* (33), 11745-11755.
602   29.   Hu, Z. H.; Margulis, C. J., Room-temperature ionic liquids: Slow dynamics,
603   viscosity, and the red edge effect. *Accounts Chem. Res.* **2007,** *40* (11), 1097-1105.
604   30.   Santiago, R.; Lemus, J.; Moreno, D.; Moya, C.; Larriba, M.; Alonso-Morales,
605   N.; Gilarranz, M. A.; Rodríguez, J. J.; Palomar, J., From kinetics to equilibrium control
606   in CO2 capture columns using Encapsulated Ionic Liquids (ENILs). *Chemical*
607   *Engineering Journal* **2018,** *348*, 661-668.
608   31.   Palomar, J.; Lemus, J.; Alonso-Morales, N.; Bedia, J.; Gilarranz, M. A.;
609   Rodriguez, J. J., Encapsulated ionic liquids (ENILs): from continuous to discrete liquid
610   phase. *Chemical Communications* **2012,** *48* (80), 10046-10048.
611   32.   Lemus, J.; Palomar, J.; A. Gilarranz, M.; J. Rodriguez, J., Characterization of
612   Supported Ionic Liquid Phase (SILP) materials prepared from different supports.
613   *Adsorption* **2011,** *17*, 561-571.
614   33.   Thomassen, P.; Kunov-Kruse, A. J.; Mossin, S.; Kolding, H.; Kegns, S.;
615   Riisager, A.; Fehrmann, R., Separation of Flue Gas Components by SILP (Supported
616   Ionic Liquid-Phase) Absorbers. In *Molten Salts and Ionic Liquids 18*, Reichert, W. M.;
617   Mantz, R. A.; Trulove, P. C.; Ispas, A.; Fox, D. M.; Mizuhata, M.; DeLong, H. C.;
618   Bund, A., Eds. 2012; Vol. 50, pp 433-442.
619   34.   Mehnert, C. P.; Cook, R. A.; Dispenziere, N. C.; Afeworki, M., Supported Ionic
620   Liquid Catalysis − A New Concept for Homogeneous Hydroformylation Catalysis.
621   *Journal of the American Chemical Society* **2002,** *124* (44), 12932-12933.
622   35.   Riisager, A.; Fehrmann, R.; Haumann, M.; Wasserscheid, P., Supported Ionic
623   Liquid Phase (SILP) catalysis: An innovative concept for homogeneous catalysis in
624   continuous fixed-bed reactors. *European Journal of Inorganic Chemistry* **2006,** (4), 695-
625   706.
626   36.   Fehrmann, R.;   Riisager, A.; Haumann, M., *Supported Ionic Liquids:*
627   *Fundamentals and Applications*. 2014; p 1-474.
628   37.   Romanos, G. E.; Schulz, P. S.; Bahlmann, M.; Wasserscheid, P.; Sapalidis, A.;
629   Katsaros, F. K.; Athanasekou, C. P.; Beltsios, K.; Kanellopoulos, N. K., CO2 Capture
630   by Novel Supported Ionic Liquid Phase Systems Consisting of Silica Nanoparticles
631   Encapsulating Amine-Functionalized Ionic Liquids. *The Journal of Physical Chemistry*
632   *C* **2014,** *118* (42), 24437-24451.
633   38.   Riisager, A.; Jørgensen, B.; Wasserscheid, P.; Fehrmann, R., First application of
634   supported ionic liquid phase (SILP) catalysis for continuous methanol carbonylation.
635   *Chemical Communications* **2006,** (9), 994-996.
636   39.   Wang, H. B.; Hu, Y.-L.; Li, D.-J., Facile and efficient Suzuki–Miyaura coupling
637   reaction of aryl halides catalyzed by Pd2(dba)3 in ionic liquid/supercritical carbon
638   dioxide biphasic system. *J. Mol. Liq.* **2016,** *218*, 429-433.
639   40.   Hu, Y. L.; Wu, Y. P.; Lu, M., Co (II)-C12 alkyl carbon chain multi-functional
640   ionic liquid immobilized on nano-SiO2 nano-SiO2@CoCl3-C12IL as an efficient
641   cooperative catalyst for C–H activation by direct acylation of aryl halides with aldehydes.
642   *Appl. Organomet. Chem.* **2018,** *32* (2), e4096.

643   41.   Yao, N.; Lu, M.; Liu, X. B.; Tan, J.; Hu, Y. L., Copper-doped mesoporous silica
644   supported dual acidic ionic liquid as an efficient and cooperative reusability catalyst for
645   Biginelli reaction. *J. Mol. Liq.* **2018,** *262*, 328-335.
646   42.   Hu, Y. L.; Zhang, R. L.; Fang, D., Quaternary phosphonium cationic ionic
647   liquid/porous metal–organic framework as an efficient catalytic system for cycloaddition
648   of carbon dioxide into cyclic carbonates. *Environmental Chemistry Letters* **2019,** *17* (1),
649   501-508.
650   43.   Jin, T.; Dong, F.; Liu, Y.; Hu, Y. L., Novel and effective strategy of dual bis
651   (trifluoromethylsulfonyl) imide imidazolium ionic liquid immobilized on periodic
652   mesoporous organosilica for greener cycloaddition of carbon dioxide to epoxides. *New J.*
653   *Chem.* **2019,** *43* (6), 2583-2590.
654   44.   Lemus, J.; Bedia, J.; Moya, C.; Alonso-Morales, N.; A Gilarranz, M.; Palomar,
655   J.; J Rodriguez, J., Ammonia Capture from Gas Phase by Encapsulated Ionic Liquids
656   (ENILs). *RSC Advances* **2016,** *6*, 61650-61660.
657   45.   Lemus, J.; Da Silva, F. A. F.; Palomar, J.; Carvalho, P. J.; Coutinho, J. A. P.,
658   Solubility of carbon dioxide in encapsulated ionic liquids. *Separation and Purification*
659   *Technology* **2018,** *196*, 41-46.
660   46.   Moya, C.; Alonso-Morales, N.; Gilarranz, M. A.; Rodriguez, J. J.; Palomar, J.,
661   Encapsulated Ionic Liquids for CO_2 Capture: Using 1-Butyl-methylimidazolium Acetate
662   for Quick and Reversible CO_2 Chemical Absorption. *Chemphyschem* **2016,** *17* (23),
663   3891-3899.
664   47.   Moya, C.; Alonso-Morales, N.; de Riva, J.; Morales-Collazo, O.; Brennecke, J.
665   F.; Palomar, J., Encapsulation of Ionic Liquids with an Aprotic Heterocyclic Anion
666   (AHA-IL) for CO_2 Capture: Preserving the Favorable Thermodynamics and Enhancing
667   the Kinetics of Absorption. *The Journal of Physical Chemistry B* **2018,** *122* (9), 2616-
668   2626.
669   48.   Santiago, R.; Lemus, J.; Moya, C.; Moreno, D.; Alonso-Morales, N.; Palomar,
670   J., Encapsulated Ionic Liquids to Enable the Practical Application of Amino Acid-Based
671   Ionic Liquids in CO_2 Capture. *ACS Sustainable Chemistry & Engineering* **2018,** *6* (11),
672   14178-14187.
673   49.   Buchel, G.; Unger, K. K.; Matsumoto, A.; Tsutsumi, K., A novel pathway for
674   synthesis of submicrometer-size solid core/mesoporous shell silica spheres. *Advanced*
675   *Materials* **1998,** *10* (13), 1036-1038.
676   50.   Alonso-Morales, N.; Gilarranz, M. A.; Palomar, J.; Lemus, J.; Heras, F.;
677   Rodriguez, J. J., Preparation of hollow submicrocapsules with a mesoporous carbon shell.
678   *Carbon* **2013,** *59*, 430-438.
679   51.   Alonso-Morales, N.; Ruiz-Garcia, C.; Palomar, J.; Heras, F.; Calvo, L.;
680   Rodriguez, J. J.; Gilarranz, M. A., Hollow Nitrogen- or Boron-Doped Carbon
681   Submicrospheres with a Porous Shell: Preparation and Application as Supports for
682   Hydrodechlorination Catalysts. *Industrial & Engineering Chemistry Research* **2017,** *56*
683   (27), 7665-7674.
684   52.   Baukal, C. E.; Eleazer, P. B., Quantifying NOx for Industrial Combustion
685   Processes. *Journal of the Air & Waste Management Association* **1998,** *48* (1), 52-58.
686   53.   Sousa, J. P. S.; Pereira, M. F. R.; Figueiredo, J. L., NO oxidation over nitrogen
687   doped carbon xerogels. *Applied Catalysis B: Environmental* **2012,** *125*, 398-408.
688   54.   Kunov-Kruse, A. J.; Thomassen, P.; Mossin, S. L.; Riisager, A.; Fehrmann, R.,
689   Absorption and oxidation of NO in 1-butyl-3-methylimidazolium based ionic liquids -
690   mechanism of reaction. *Abstracts of Papers of the American Chemical Society* **2014,** *247*.

23

691　55.　　Mochida, I.; Kisamori, S.; Hironaka, M.; Kawano, S.; Matsumura, Y.;
692　Yoshikawa, M., Oxidation of NO into NO2 over Active Carbon Fibers. *Energy & Fuels*
693　**1994,** *8* (6), 1341-1344.
694　56.　　Mochida, I.; Kawabuchi, Y.; Kawano, S.; Matsumura, Y.; Yoshikawa, M., High
695　catalytic activity of pitch-based activated carbon fibres of moderate surface area for
696　oxidation of NO to NO2 at room temperature. *Fuel* **1997,** *76* (6), 543-548.
697　57.　　Guo, Z.; Xie, Y.; Hong, I.; Kim, J., *Catalytic oxidation of NO to NO2 on activated*
698　*carbon*. 2001; Vol. 42, p 2005-2018.
699　58.　　Ruggeri, M. P.; Nova, I.; Tronconi, E., Experimental Study of the NO Oxidation
700　to NO2 Over Metal Promoted Zeolites Aimed at the Identification of the Standard SCR
701　Rate Determining Step. *Top. Catal.* **2013,** *56* (1), 109-113.
702　59.　　Atkins, P.; de Paula, J., *Atkins' Physical Chemistry*. 9th ed.; OUP Oxford: 2010.
703　60.　　Hubbe, M.; D Smith, R.; Zou, X.; Katuscak, S.; Potthast, A.; Ahn, K.,
704　*Deacidification of Acidic Books and Paper by Means of Non-aqueous Dispersions of*
705　*Alkaline Particles: A Review Focusing on Completeness of the Reaction*. 2017; Vol. 12,
706　p 4410-4477.
707　61.　　Lyon, R. K.; Cole, J. A.; Kramlich, J. C.; Chen, S. L., The selective reduction of
708　SO3 to SO2 and the oxidation of NO to NO2 by methanol. *Combustion and Flame -*
709　*COMBUST FLAME* **1990,** *81* (1), 30-39.
710　62.　　Zamansky, V. M.; Ho, L. O. C.; Maly, P. M.; Seeker, W. R., Oxidation of NO to
711　NO2 by Hydrogen Peroxide and its Mixtures with Methanol in Natural Gas and Coal
712　Combustion Gases. *Combust. Sci. Technol.* **1996,** *120* (1-6), 255-272.
713　63.　　Rasmussen, C. L.; Wassard, K. H.; Dam-Johansen, K.; Glarborg, P., Methanol
714　oxidation in a flow reactor: Implications for the branching ratio of the CH3OH+ OH
715　reaction. *International Journal of Chemical Kinetics* **2008,** *40* (7), 423-441.
716　64.　　Taylor, P.; Cheng, L.; Dellinger, B., The influence of nitric oxide on the oxidation
717　of methanol and ethanol. *Combustion and Flame - COMBUST FLAME* **1998,** *115*, 561-
718　567.
719　65.　　Alzueta, M. U.; Bilbao, R.; Finestra, M., Methanol Oxidation and Its Interaction
720　with Nitric Oxide. *Energy & Fuels* **2001,** *15* (3), 724-729.
721　66.　　Xiao, C.-X.; Yan, N.; Zou, M.; Hou, S.-C.; Kou, Y.; Liu, W.; Zhang, S., NO2-
722　catalyzed deep oxidation of methanol: Experimental and theoretical studies. *Journal of*
723　*Molecular Catalysis A: Chemical* **2006,** *252* (1), 202-211.
724　67.　　Artioli, N.; Lobo, R. F.; Iglesia, E., Catalysis by Confinement: Enthalpic
725　Stabilization of NO Oxidation Transition States by Micropororous and Mesoporous
726　Siliceous Materials. *The Journal of Physical Chemistry C* **2013,** *117* (40), 20666-20674.
727　68.　　Loiland, J. A.; Lobo, R. F., Low temperature catalytic NO oxidation over
728　microporous materials. *Journal of Catalysis* **2014,** *311*, 412-423.

24
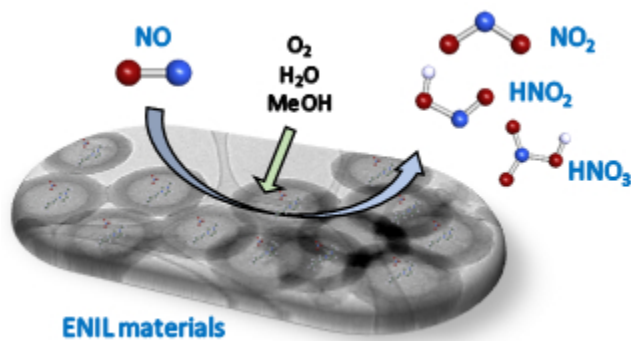
Methanol promoted oxidation of NO using Encapsulated Ionic Liquids (ENILs)

84x47mm (96 x 96 DPI)